

SLAC - PUB - 3564
January 1985
(T/E)

HELICITY AMPLITUDES IN $e^+e^- \rightarrow e^+e^-\gamma\gamma$
DOUBLE BREMSSTRAHLUNG*

BRUCE K. SAWHILL

Stanford Linear Accelerator Center

Stanford University, Stanford, California, 94305

ABSTRACT

A compact form for the helicity amplitudes of double bremsstrahlung is presented, utilizing a recently developed method of representing free photon polarizations which produces very compact results. The application as a polarization monitor in a colliding beam machine such as the SLC is discussed.

Submitted to *Physical Review D*

* Work supported by the Department of Energy, contract DE - AC03 - 76SF00515.

1. Introduction

Double bremsstrahlung has become interesting recently as a luminosity monitor for colliding beam machines because it is a process that is both uniquely identifiable and measurable without interfering with the particle beams. It is also polarization dependent, a property that could be of use in the next generation of colliding beam machines. Even though total cross-sections have been calculated¹⁻⁵ using various approximations such as soft photons, photon-fermion collinearity, and very high beam energies, no calculation yet exists that is broken down into helicity amplitudes. An excellent review of the field of bremsstrahlung calculations is the one by Baier, Kuraev, et al.⁶

Until recently, the only way to obtain helicity dependent cross-sections was by the standard method of picking an arbitrary polarization vector, inserting helicity projection operators, and calculating traces of the entire set of matrix element products that contribute. Even though the end results are often compact, a considerable degeneracy of contributing diagrams and a large number of gamma-matrices in each process cause an overwhelming proliferation of terms in intermediate expressions. It is possible to evaluate these traces using a symbolic Dirac algebra program such as REDUCE or MACSYMA, but the results are so opaque as to be useless.

In a series of papers written from 1981-84,⁷⁻¹² a number of collaborating authors (the CALKUL group) have developed a method of calculating bremsstrahlung processes which involve free photons radiated from non-loop fermion lines. The central feature of their method is the choice of a representation for the photon polarization that is a function of the external fermion momenta. This causes a large degree of simplification because only a subset of diagrams contributes to

each choice of particle helicities. In effect, this method uses gauge cancellations at the matrix element level so as to avoid very large intermediate expressions for probability amplitudes.

In this paper, this method is presented in Chapter 2, double bremsstrahlung is discussed in Chapter 3, and the method is applied to d.b. in Chapter 4, resulting in reasonably compact expressions for probabilities. Chapter 5 is a discussion of the applications of double bremsstrahlung.

2. Method

The method of calculating matrix elements used in this paper was developed specifically for high-energy QED (massless fermion) bremsstrahlung processes by the CALKUL collaboration.⁸ This method has been generalized to massless non-Abelian gauge theories,¹³ and has also been extended by the author of this paper to utilize the Weyl spinor algebra algorithm developed by Farrar and Neri¹⁴ for use in problems with both collinear particles and bremsstrahlung. The key argument utilized by the CALKUL collaboration is the choice of polarization for the free photon line(s). Consider a contiguous fermion line that ends in two continuum states. Label the momenta of the two ends p_- and p_+ . The radiated photon momenta are labelled k_i , and $p_+^2 = p_-^2 = k_i^2 = 0$. One chooses the representation of the parallel and perpendicular components of ϵ^i as follows:

$$[\epsilon_\mu^i]^\parallel = N[(p_+ k_i) p_{-\mu} - (p_- k_i) p_{+\mu}]$$

and

$$[\epsilon_\mu^i]^\perp = N[\epsilon_{\mu\alpha\beta\gamma} p_+^\alpha p_-^\beta k_i^\gamma] \quad (2.1)$$

where

$$(\epsilon^{\parallel})^2 = (\epsilon^{\perp})^2 = -1, \quad (2.2)$$

$$(k\epsilon^{\parallel})_i = (k\epsilon^{\perp})_i = (\epsilon^{\parallel}\epsilon^{\perp})_i = 0. \quad (2.3)$$

and

$$N_{q_{+,-}}^{k_i} = [2(p_+p_-)(p_-k_i)(p_+k_i)]^{-\frac{1}{2}} \quad (2.4)$$

One can then construct the Dirac product for circularly polarized photons:

$$\not{e}^{\pm} = \frac{-1}{2\sqrt{2}} N [\not{k} \not{p}_- \not{p}_+ (1 \pm \gamma_5) - \not{p}_- \not{p}_+ \not{k} (1 \mp \gamma_5) \mp 2(p_+p_-) \not{k} \gamma_5] \quad (2.5)$$

$$\text{where } \epsilon_{\pm} = \frac{1}{\sqrt{2}} (\epsilon^{\parallel} \pm i\epsilon^{\perp}).$$

The third term can be dropped because of gauge invariance. This choice of polarization representation causes the following simplifications if the photon line in question is adjacent to one of the continuum ends of a fermion line. One of the two terms of \not{e} will vanish by the massless Dirac equation $\bar{\Psi}(p_{\pm})\not{p}_{\pm} = 0$. The polarization term that remains will further simplify. Consider the product

$$\frac{\bar{\Psi}(p_-)\not{e}_{(k,p_-,p_+)}^{\pm}(\not{p}_- + \not{k}) \dots}{(p_- + k)^2}. \quad (2.6)$$

Using the massless Dirac equation twice yields

$$\frac{-N\bar{\Psi}(p_-)\not{p}_+(\not{p}_- + \not{k})(1 \pm \gamma_5) \dots}{2\sqrt{2}}. \quad (2.7)$$

In many bremsstrahlung processes, one must consider the same free photon

being emitted from different fermion lines. A photon has only two polarizations and hence any two sets of polarization vectors must be related by a phase.

$$\epsilon_\mu^\pm(p_+, p_-, k) = e^{i\phi^\pm} \epsilon_\mu'^\pm(p_+ l, p_- l, k) + \Lambda_\pm k_\mu. \quad (2.8)$$

Since the different fermionic currents are separately conserved, Λ_\pm is a constant and irrelevant. Relative phases of the different representations are given by the dot products of the respective ϵ_μ .

The previously described method has been used to calculate a variety of matrix elements in QED, such as $e^+e^- \rightarrow \gamma\gamma\gamma$, $\mu^+\mu^-\gamma$, $e^+e^-\gamma^8$, $\gamma\gamma\gamma\gamma^9$, and $e^+e^-e^+e^-$ ¹⁰.

3. Matrix Elements

3.1 FNEYMAN DIAGRAMS

There are 40 Feynman diagrams that contribute to tree-level $e^+e^- \rightarrow e^+e^-\gamma\gamma$ double bremsstrahlung. In this section the matrix elements for the complete process are presented as a function of the helicities of the fermions and photons. The Feynman diagrams fall into 12 gauge invariant subsets which can be further reduced to four different topological classes. These four classes are shown in Figure 1. The entire set of matrix elements can be obtained from the helicity amplitudes of one diagram from each class by a prescription for permutations. These four topological classes are enumerated as follows:

Type 1: Processes in which both photons are emitted from the same leg of the same fermion line, of the form

$$\frac{\bar{u}(p_3)\gamma_\mu(p_1 - k_1 - k_2)\epsilon_2(p_1 - k_1)\epsilon_1 u(p_1)\bar{v}(p_2)\gamma^\mu v(p_4)}{(p_1 - k_1 - k_2)^2(p_1 - k_1)^2(p_2 - p_4)^2} \quad (3.1)$$

Type 2: Processes in which the two free photons are emitted from opposite legs of the same fermion line, of the form

$$\frac{\bar{u}(p_3)\epsilon_2(p_3 + k_2)\gamma_\mu(p_1 - k_1)\epsilon_1 u(p_1)\bar{v}(p_2)\gamma^\mu v(p_4)}{(p_3 + k_2)^2(p_1 - k_1)^2(p_2 - p_4)^2} \quad (3.2)$$

Type 3: Processes in which the two free photons are emitted from different fermion lines such that both of them are emitted either on the incoming legs or the outgoing legs:

$$\frac{\bar{u}(p_3)\gamma_\mu(p_1 - k_1)\epsilon_1 u(p_1)\bar{v}(p_2)\epsilon_2(p_2 - k_2)\gamma^\mu v(p_4)}{(p_1 - k_1)^2(p_2 - k_2)^2(p_2 - p_4)^2} \quad (3.3)$$

Type 4: Processes in which the two free photons are emitted from different fermion lines, one from an incoming leg, one from an outgoing leg:

$$\frac{\bar{u}(p_3)\gamma_\mu(p_1 - k_1)\epsilon_1 u(p_1)\bar{v}(p_2)\gamma^\mu(-p_4 + k_2)\epsilon_2 v(p_4)}{(p_1 - k_1)^2(-p_4 + k_2)^2(p_1 - k_1 - p_3)^2} \quad (3.4)$$

3.2 SYMMETRIES

The symmetry transformations that are used to obtain the remaining graphs are of three kinds. One can utilize charge conjugation, time reversal, and rotation of t-channel to s-channel. These operations in conjunction with momentum relabelling produce all of the contributing helicity amplitudes. Any product of

these three operations is also a legitimate symmetry transformation. One must take care to keep track of the changes in helicity relationships caused by these transformations. Notice that it is not possible to transform Eq. 2 into Eq. 3 because it involves a twist about the virtual photon line and hence is not a rigid symmetry operation that preserves topological relationships.

For double bremsstrahlung, the 8 possible product transformations that can be constructed from the three basic symmetry transformations must be multiplied by a factor of two to account for photon exchange. For the processes of Types 2,3, and 4, there is a degeneracy among the symmetry transformations, producing only 8 possible permutations of the basic topology instead of 16.

The basic set of matrix elements and the actual substitutions required to obtain the remaining ones are presented in the next chapter.

4. Results

The helicity dependent matrix elements of the four basic types of Feynman graphs are presented with the following conventions:

1. The processes are calculated in the t channel.
2. The phase factor of the matrix element is normalized to zero for the case when both photons are emitted by the contiguous electron line (labelled $p_{1,3}$).
3. The matrix element for a given topology of Feynman graph and its associated set of helicities is represented as such: $M_{T,x}(h_{p_1}, h_{p_2}, h_{p_3}, h_{p_4}, h_{k_1}, h_{k_2})$, where T specifies the type of graph and x specifies the specific sub-amplitude within that type. The helicity of the electron line will be defined as + with no loss of generality, as all of the derived quantities are invariant under helicity conjugation in massless QED.

4. Some definitions for helicity projection operators:

$$\left\{ \begin{array}{l} u_{\pm} = u \frac{1}{2} (1 \pm \gamma_5) \\ v_{\pm} = \frac{1}{2} (1 \mp \gamma_5) v \\ \bar{u}_{\pm} = \frac{1}{2} (1 \mp \gamma_5) \bar{u} \\ \bar{v}_{\pm} = \bar{v} \frac{1}{2} (1 \pm \gamma_5) \end{array} \right\} \quad (4.1)$$

5. Some conventions for combinations of momenta;

$$\left\{ \begin{array}{l} x_{11} = p_1 - k_1 \\ x_{112} = p_1 - k_1 - k_2 \\ x_{32} = p_3 + k_2 \\ x_{22} = -p_2 + k_2 \\ x_{42} = -p_4 - k_2 \end{array} \right\} \quad (4.2)$$

Consider a matrix element of type 1. Choosing a set of helicities and inserting explicit representations for the photon polarizations gives

$$M_1(+, +, +, +, -, -)$$

$$= -N^2 \frac{\bar{u}(p_3)(1 - \gamma_5)\gamma_{\mu}(p_{112})(p_3 p_1 k_2)(p_{11})(p_3 p_1 k_1)u(p_1)\bar{v}(p_2)\gamma^{\mu}(1 - \gamma_5)v(p_4)}{(p_1 - k_1 - k_2)^2(p_4 - p_2)^2(p_1 - k_1)^2} \quad (4.3)$$

where N is the normalization factor of the polarization vectors, and all of the expressions containing γ_5 have been condensed as much as possible. At this point it is useful to reverse the order of the two Dirac strings in the above product and to insert a factor $\bar{v}(p_4)u(p_3)$ between them while dividing by the

same object. This creates one string out of two separate Dirac strings and makes the connection between the helicities of the two fermion lines more transparent. It is important to notice that the insertion factor used above would have to be different if the helicity of the $p_{2,4}$ line was $-$. In such a case, the insertion factor must be modified by including (and dividing by) an object that will change the sign of γ_5 . Conventionally, a four-momentum contracted with a gamma-matrix is inserted. Inserting the previously mentioned factor yields

$$\mathcal{M}_{1,1}(+, +, +, +, -, -) =$$

$$\frac{-2N^2}{D} \frac{\bar{v}(p_2)\gamma^\mu p_4 p_3 \gamma_\mu (1 \pm \gamma_5)(\not{p}_{112})\not{p}_3 \not{p}_1 \not{k}_2 (\not{p}_{11})(\not{p}_3 \not{p}_1 \not{k}_1) u(p_1)}{\bar{v}(p_4)u(p_3)} \quad (4.4)$$

Squaring and simplifying yields

$$|\mathcal{M}_{1,1}(+, +, +, +, -, -)|^2 = \frac{128N^2(p_1 k_1)^2(p_4 p_3)(p_1 p_3)}{D^2} \frac{Tr}{4} \left\{ \begin{aligned} & p_2(1 + \gamma_5)(\not{p}_{112})(\not{p}_3 \not{p}_1 \not{k}_2) \\ & \times (\not{p}_{11})\not{p}_3(\not{p}_{11})(\not{k}_2 \not{p}_1 \not{p}_3)(\not{p}_{112}) \end{aligned} \right\} \quad (4.5)$$

The trace is evaluated by utilizing REDUCE and the normalizations for the polarization vectors are expressed explicitly, yielding:

$$|\mathcal{M}_{1,1}(+, +, +, +, -, -)|^2 = \frac{(p_1 k_1)(p_4 p_3)}{(p_3 k_1)(p_3 k_2)(p_4 - p_2)^4 x_{11}^4 x_{112}^4} \left\{ \begin{aligned} & x_{11}^2 x_{112}^2 (k_2 p_3)(p_3 p_2) \\ & -2x_{11}^2 (x_{112} p_3)(x_{112} p_2)(k_2 p_3) \\ & -2x_{112}^2 (x_{11} k_2)(x_{11} p_3)(p_3 p_2) \\ & + 4(x_{11} k_2)(x_{11} p_3)(x_{112} p_3)(x_{112} p_2). \end{aligned} \right\} \quad (4.6)$$

The remaining nine matrix elements are calculated by the same procedure

and are summarized in Appendix A. Because of the representations used for the photon polarizations, some graphs pick up minus signs at the amplitude level. Graphs of types 2 and 3 have intrinsic minus signs, as do graphs of type 1 in which the helicity of the photon labelled by k_2 is +. The method of this paper was checked by summing the t-channel helicity probabilities with forward-backward photons and comparing with the result obtained by conventional trace methods,⁵ obtaining complete agreement.

The phase factors for the amplitudes are normalized such that $e^{i\phi} = 1$ when both of the free photons are emitted from the $p_{1,3}$ electron line in the t channel. When symmetry operations are performed on the amplitudes to obtain the results of the other Feynman graphs, phases are induced. If a photon labelled k_i is emitted from a fermion line labelled by p_l and p_m , the phase factor is given by

$$(N_{p_{1,3}}^{k_i} N_{p_{l,m}}^{k_i}) Tr\{p_1 p_3 k_i p_l p_m k_i (1 + \gamma_5)\}. \quad (4.7)$$

This gives

$$Re[e^{i\phi}] = N_{p_{1,3}}^{k_i} N_{p_{l,m}}^{k_i} \left\{ \begin{array}{l} (p_m k_i)(p_l k_i)(p_1 k_i) - (p_m p_1)(p_l k_i)(p_3 k_i) \\ \quad - (p_m k_i)(p_l p_3)(p_1 k_i) + (p_m k_i)(p_l p_i)(p_3 k_i) \end{array} \right\} \quad (4.8)$$

and $Im[e^{i\phi}] =$

$$2i N_{1,3}^i N_{l,m}^i [(p_m k_i) \epsilon_{\alpha\beta\gamma\delta} p_l^\alpha p_3^\beta p_1^\gamma k_i^\delta - (p_l k_i) \epsilon_{\alpha\beta\gamma\delta} p_m^\alpha p_3^\beta p_1^\gamma k_i^\delta], \quad (4.9)$$

where the N are given by Eq. A. It is readily seen that $e^{i\phi} = 1$ for $p_l = p_1$ and $p_m = p_3$, as expected.

4.1 SYMMETRY TRANSFORMATIONS

The three symmetry transformations and their effects on momentum and helicity labelling are enumerated below.

1. Charge conjugation leaves unchanged the relative helicity of the photon and the line that emits it. Momenta are relabelled as such: $(p_1 \leftrightarrow p_2, p_3 \leftrightarrow p_4)$. Finally, all internal momenta change sign, producing no net effect in this process because each graph is bilinear in internal momenta.
2. Time reversal reverses the relative helicity of the photon and the line that emits it. Momenta are relabelled as such: $(p_1 \leftrightarrow -p_3, p_2 \leftrightarrow -p_4)$. All internal momenta change sign, producing no net effect as in charge conjugation.
3. Rotation of t-channel into s-channel leaves unchanged p_1 and p_4 and the relative helicities of photons emitted from those lines. Other momenta change as such: $(p_2 \leftrightarrow -p_3)$. The relative helicity of a photon emitted from line p_2 or p_3 is reversed, as is the sign of internal momenta. An overall minus sign for the amplitude is induced because of fermion statistics.

5. Discussion and Applications

In the last section, it was shown how to obtain the matrix elements for all forty graphs and 112 associated helicity amplitudes that contribute to double-bremsstrahlung at tree level. For any given application, it is unlikely that one needs to consider this number of amplitudes. This is because the amplitudes have a very strongly peaked structure in space and the interference terms between amplitudes with peaks in different places are minuscule.

The application being considered here is the use of a double-bremsstrahlung luminosity monitor in the Stanford Linear Collider (SLC) that will be able to monitor the amount and type of polarization present in the colliding beams. The SLC will not be a polarized beam machine at first, but it is planned as a later modification. Since the luminosity of the SLC is to be quite low compared to that of a LEP-type storage ring, it is essential to have a luminosity and polarization monitor that does not interfere with the beams themselves in such a way as to reduce luminosity.

The kind of detector used in the SLC would be a standard combination of scintillator and phototube. The reason for using double bremsstrahlung instead of single bremsstrahlung is that it is possible to build a monitor that selects out this process with extreme accuracy. This can be done by placing a luminosity monitor on each side of the interaction region and connecting their outputs to a coincidence circuit that eliminates all other processes that do not give forward-backward simultaneous photons, such as single bremsstrahlung, etc.

By inspecting the matrix elements of the Feynman graphs given in the last chapter, it is possible to see that a large number of them will not contribute significantly to the events that would be detected by the SLC monitor. At very relativistic energies, the collinearity of the photons with their respective fermion lines is very large. This is the quantum analogue of the well-known classical phenomenon of the narrowing of the radiation cone. It can be seen to occur in the matrix elements because the denominators of the form pk become very small when k becomes very nearly parallel to p .

The fact that this denominator is small also means that the sub-process (the process that remains when the free photons are amputated) is very close to

being on shell in the region where the d.b. amplitude is large. This causes a kind of factorization in which the helicity dependence of the sub-process is preserved when photons are emitted, as the emission of photons does not change the helicity of the sub-graph in the relativistic limit. Hence one can study Møller and Bhabha scattering without actually interfering with the fermions. The formulae for these processes are much simpler than the ones for double bremsstrahlung and they can be used as guides to decide which matrix elements of d.b. are significant. Before analyzing the amputated processes, it is more useful to use the coarser sieve of collinearity to reduce the hordes of matrix elements.

One can immediately discard graphs of Type 1 because they emit both photons from the same side of the same fermion line, hence the photons will both be strongly peaked in the direction of that fermion and will not be registered because of the coincidence circuit. Graphs of Type 2 are tempting to throw out also, and this is a valid thing to do if one is in the t channel, however, if one rotates to the s channel, the photons will be emitted in opposite directions. A further temptation exists to throw the s channel graphs out because of the huge denominator, but it is advisable to wait. It is not possible *a priori* to throw out all of the graphs of Types 3 and 4 because there are some that are both t channel and that have photons emitted from different fermion lines. A careful inspection shows that one is left with 8 graphs that display anticollinearity.

At this point it is useful to examine the sub-process graphs of double bremsstrahlung. There are two graphs that contribute, one t channel and the other s channel. Each one of these has two possible helicity combinations. The helicity probabilities are tabulated below, reproducing values given in the literature.¹⁵

$$\left\{ \begin{array}{l} |\mathcal{M}_1(+, +, +, +)|^2 = \frac{8(p_1 p_2)(p_3 p_4)}{(p_1 - p_3)^2} \\ |\mathcal{M}_1(+, -, +, -)|^2 = \frac{8(p_1 p_4)(p_3 p_2)}{(p_1 - p_3)^2} \\ |\mathcal{M}_2(+, -, +, -)|^2 = \frac{8(p_1 p_4)(p_2 p_3)}{(p_1 + p_2)^2} \\ |\mathcal{M}_2(+, -, -, +)|^2 = \frac{8(p_1 p_3)(p_2 p_4)}{(p_1 + p_2)^2} \end{array} \right\} \quad (5.1)$$

To evaluate the relative significance of these helicity probabilities, it is essential to choose some specific kinematics. The colliding electron and positron beams of energy E are represented by p_1 and p_2 , respectively. The final state electron and positron are represented by p_3 and p_4 , respectively. By momentum conservation, they scatter back-to-back with energy E and a relative angle θ from their respective initial states. The contributions to the cross-section are tabulated below in terms of the helicity combinations responsible for each term. The constant $\frac{\alpha^2}{8E}$ multiplying each term has been dropped.

$$\left\{ \begin{array}{l} (+, +, +, +)_{t\text{-chan.}} \rightarrow \frac{1}{\sin^4(\frac{\theta}{2})} \\ (+, -, +, -)_{t\text{-chan.}} \rightarrow \frac{\cos^4(\frac{\theta}{2})}{\sin^4(\frac{\theta}{2})} \\ (+, -, +, -)_{\text{Interf}} \rightarrow \frac{-2\cos^4(\frac{\theta}{2})}{\sin^2(\frac{\theta}{2})} \\ (+, -, +, -)_{s\text{-chan.}} \rightarrow \frac{(1 + \cos\theta)^2}{2} \\ (+, -, -, +)_{s\text{-chan.}} \rightarrow \frac{(1 - \cos\theta)^2}{2} \end{array} \right\} \quad (5.2)$$

The sum of all of the terms enumerated above reproduces the ultra-relativistic cross-section given in standard textbooks.¹⁶ By inspection, it is obvious that the t-channel probabilities have the famous Rutherford $\sin^4(\frac{\theta}{2})$ denominator and

hence contribute overwhelmingly to the cross-section in the forward scattering cone. From this result it would seem to safe to throw away all s-channel graphs in double bremsstrahlung processes, because there is a region of high total cross-section where their contribution is negligible. The quantity being considered here is the polarization asymmetry, defined as

$$A_{LR} = \frac{\sigma_{LL} - \sigma_{LR}}{\sigma_{LL} + \sigma_{LR}} \quad (5.3)$$

where σ_{LL} is proportional to the probability given by $|\Sigma \mathcal{M}(+, +, \dots)|^2$ and σ_{LR} is proportional (by the same factor as σ_{LL}) to $|\Sigma \mathcal{M}(+, -, \dots)|^2$. When constructing the polarization asymmetry, it is inconsistent to discard contributions from s-channel graphs because terms of leading order in θ cancel. To make this more clear, it is instructive to expand the terms in the cross-section above as power-series in θ and to observe the dependence of the polarization asymmetry. This is easily done using MACSYMA, and the results for various processes are given below:

$$A_{LR}(e^+e^- \rightarrow e^+e^-) = \frac{1}{2}\theta^2 + \frac{1}{48}\theta^4 - \frac{29}{720}\theta^6 + \dots \quad (5.4)$$

$$A_{LR}(e^- \mu^- \rightarrow e^- \mu^-) = \frac{1}{4}\theta^2 + \frac{1}{96}\theta^4 - \frac{13}{2880}\theta^6 + \dots \quad (5.5)$$

The asymmetry for the process $e^-e^- \rightarrow e^-e^-$ is the same as for $e^+e^- \rightarrow e^+e^-$ because of crossing symmetry. The process $e^+e^- \rightarrow \mu^+\mu^-$ has an asymmetry of 1 because the only contribution to the cross-section comes from opposite helicities of the incoming particles. It can be seen from the expansions above that it is

important to consider the s channel in e^+e^- scattering because the leading order asymmetry differs by a factor of 2 from the t channel ($e^-\mu^-$). This factor of 2 in the leading term comes from the interference term between the s-channel and t-channel graphs. This is readily seen by expanding the contributions of the different terms in e^+e^- scattering:

t-channel squared:

$$\frac{1}{4}\theta^2 + \frac{7}{96}\theta^4 - \frac{43}{2880}\theta^6 + \dots \quad (5.6)$$

s-channel squared:

$$-\frac{1}{32}\theta^4 + \frac{1}{192}\theta^6 + \dots \quad (5.7)$$

Interference term:

$$\frac{1}{4}\theta^2 - \frac{1}{48}\theta^4 - \frac{11}{360}\theta^6 + \dots \quad (5.8)$$

It can be concluded that annihilation effects must be taken into consideration to properly evaluate the asymmetry effects in double-bremsstrahlung, even when the scattering angles between the fermions are very small. Therefore the graphs that are of interest are the same as the ones selected by anticollinearity. It is not necessary to include graphs where the photons are exchanged because that has the effect of producing two enormous denominators, hence a negligible contribution. Since the photon labels are not exchanged here, it is important to keep track of the effect symmetry transformations have on the labelling of photon lines. The convention is adopted where the photon labelled $k_1(k_2)$ is emitted from a matter(antimatter) line.

$|\Sigma M(+,+,\dots)|^2$ and $|\Sigma M(+,-,\dots)|^2$ are given by

$$|\Sigma M(+, +, \dots)|^2 = |M_{3,1}|^2 + |AM_{3,1}|^2 + |M_{4,1}|^2 + |AM_{4,1}|^2 \quad (5.9)$$

and

$$\text{and } |\Sigma M(+, -, \dots)|^2$$

$$= \left\{ \begin{array}{l} |AM_{3,2}|^2 + |CM_{2,2}|^2 + |M_{3,2}|^2 + |CBM_{2,2}|^2 \\ + |M_{4,2}|^2 + |CM_{4,2}|^2 + |AM_{4,2}|^2 + |CAM_{4,2}|^2 \\ + |CM_{4,1}|^2 + |CBM_{2,1}|^2 + |CM_{2,1}|^2 + |CAM_{4,1}|^2 \\ + |AM_{3,2}| |CM_{2,2}| \cos(\phi_1) + |M_{3,2}| |CBM_{2,2}| \cos(\phi_2) \\ + |M_{4,2}| |CM_{4,2}| \cos(\phi_3) + |AM_{4,2}| |CAM_{4,2}| \cos(\phi_4) \\ - |CM_{4,1}| |CBM_{2,1}| \cos(\phi_5) - |CM_{4,1}| |CM_{2,1}| \cos(\phi_6) \\ + |CBM_{2,1}| |CM_{2,1}| \cos(\phi_7) \end{array} \right\} \quad (5.10)$$

where the ϕ are given by

$$\left\{ \begin{array}{l} \phi_1 = \phi_{24}^2 - \phi_{12}^1 - \phi_{12}^2 \\ \phi_2 = \phi_{24}^2 - \phi_{34}^1 - \phi_{34}^2 \\ \phi_3 = \phi_{24}^2 - \phi_{12}^1 - \phi_{34}^2 \\ \phi_4 = \phi_{24}^2 - \phi_{12}^1 - \phi_{34}^2 \\ \phi_5 = \phi_{12}^1 - \phi_{34}^1 \\ \phi_6 = \phi_{34}^2 - \phi_{12}^2 \\ \phi_7 = \phi_{34}^1 + \phi_{34}^2 - \phi_{12}^1 - \phi_{12}^2 \end{array} \right\} \quad (5.11)$$

and the transformations perform the following substitutions of momenta:

$$\left\{ \begin{array}{l} AM(p_1, p_2, p_3, p_4, k_1, k_2) \rightarrow M(-p_1, -p_2, -p_3, -p_4, k_1, k_2) \\ CM(p_1, p_2, p_3, p_4, k_1, k_2) \rightarrow M(p_1, -p_3, -p_2, p_4, k_1, k_2) \\ CBM(p_1, p_2, p_3, p_4, k_1, k_2) \rightarrow M(-p_3, p_1, p_4, -p_2, k_1, k_2) \\ CAM(p_1, p_2, p_3, p_4, k_1, k_2) \rightarrow M(p_2, -p_4, -p_1, p_3, k_2, k_1) \end{array} \right\} \quad (5.12)$$

Using the above results, it would be straightforward to write a Monte Carlo routine that calculates the asymmetry or total cross-section for a given detector configuration.

The t-channel total cross-section for high-energy double bremsstrahlung has been calculated⁴, and it can be used as a guide to determine the effectiveness of an asymmetry monitor. An ideal detector covering the solid angle from the beam direction itself out to an angle $\theta = 10\frac{m_e}{E}$ would capture well over 99% of the d.b. events, producing 10-1000 events/sec, depending on the luminosity of the machine and the kinematic cuts of the detector. The asymmetry is difficult to measure because it is an effect that is attenuated by a factor of θ^2 and because it is a difference of two large numbers, both of which are subject to statistical errors that make it impossible to resolve their difference without going to extremely long integrating times. These problems make double bremsstrahlung an unlikely candidate for a polarization monitor unless a method is developed whereby the helicity of an individual photon in the GeV range can be easily measured.

5.1 FINITE MASS EFFECTS AND Z_0 EFFECTS

In any extremely relativistic process, the first mass-dependent terms that contribute to the S-Matrix elements are attenuated by a factor of $\frac{m^2}{E^2}$. For the SLC beam energy of 50 GeV, this is a factor of 10^{-10} , hence these effects are insignificant compared to the accuracy of any conceivable experiment.

One advantage of the helicity formalism used in this paper is the ease of including particles with chiral properties to mediate the interaction between the two fermion lines. If one includes Z_0 exchange via a coupling of the form $\gamma_\mu[a(1 - \gamma_5) + b(1 + \gamma_5)]$ it is clear by inspection that every d.b. matrix element will pick up a factor of a^2, ab , or b^2 . If one includes an imaginary pole in the denominator of the Z_0 propagator to describe the decay width, this will influence the matrix elements of double bremsstrahlung in that the imaginary term will combine with the imaginary part of the photon induced phase (Eq. 4.9) to give a real contribution.⁷

ACKNOWLEDGEMENTS

I would like to thank Giora Tarnopolsky for the original idea in the context of the SLC and Stan Brodsky for enlightening discussions.

REFERENCES

1. V.N. Baier and V.M. Galitsky, *Physics Letters* **13** (1964) 355
2. V.N. Baier and V.M. Galitsky, *Soviet Physics JETP* **22** (1966) 459
3. V.N. Baier and V.M. Galitsky, *JETP Letters* **2** (1965) 165
4. V.N. Baier, V.S. Fadin, and V.A. Khoze, *Soviet Physics JETP* **23** (1966) 1073
5. P. Di Vecchia and M. Greco, *Nuovo Cimento* **50** (1967) 319
6. V.N. Baier, E.A. Kuraev, V.S. Fadin, and V.A. Khoze, *Phys. Rep.* **78** (1981) 293
7. F.A. Berends, R. Kleiss, P. de Causmaecker, R. Gastmans, W. Troost, and T.T. Wu (CALKUL collaboration), *Nucl. Phys.* **B206** (1982) 61
8. P. de Causmaecker, R. Gastmans, et al., *Nucl. Phys.* **B206** (1982) 53
9. F.A. Berends, R. Kleiss, et al., *Phys. Lett.* **103B** (1981) 124
10. P. de Causmaecker, R. Gastmans, et al., *Phys. Lett.* **105B** (1981) 215
11. CALKUL collaboration (F.A. Berends, et al., *Nucl. Phys.* **B239** (1984) 382
12. CALKUL collaboration (F.A. Berends, et al.), *Nucl. Phys.* **B239** (1984) 395
13. Z. Xu, D. Zhang, and L. Chang: Preprint TUTP-84/3-Tsinghua (1984)
14. Glennys R. Farrar and Filippo Neri, *Phys. Lett.* **130B** (1983) 109
15. L.L. DeRaad, Jr. and Yee Jack Ng, *Phys. Rev.* **D10** (1974) 3440
16. J.D. Bjorken and S.D. Drell, *Relativistic Quantum Mechanics*, pp. 135-140

APPENDIX A

$$|\mathcal{M}_{1,2}(+, -, +, -, -, -)|^2 =$$

$$\frac{(p_2 p_3)(p_1 k_1)}{(p_3 k_1)(p_3 k_2)(p_4 - p_2)^4 x_{11}^4 x_{112}^4} \left\{ \begin{array}{l} x_{11}^2 x_{112}^2 (k_2 p_3)(p_4 p_3) \\ -2x_{11}^2 (x_{112} p_4)(x_{112} p_3)(k_2 p_3) \\ -2x_{112}^2 (x_{11} k_2)(x_{11} p_3)(p_4 p_3) \\ +4(x_{11} k_2)(x_{11} p_3)(x_{112} p_4)(x_{112} p_3). \end{array} \right\}$$

$$|\mathcal{M}_{1,3}(+, +, +, +, -, +)|^2 =$$

$$\frac{(p_3 p_4)(p_1 k_1)}{(p_1 k_2)(p_3 k_1)(p_4 - p_2)^4 x_{11}^4 x_{112}^4} \left\{ \begin{array}{l} x_{11}^2 x_{112}^2 (k_2 p_2)(p_3 p_1) \\ -2x_{11}^2 (x_{112} k_2)(x_{112} p_2)(p_3 p_1) \\ -2x_{112}^2 (x_{11} p_3)(x_{11} p_1)(k_2 p_2) \\ +4(x_{11} p_3)(x_{11} p_1)(x_{112} k_2)(x_{112} p_2). \end{array} \right\}$$

$$|\mathcal{M}_{1,4}(+, -, +, -, -, +)|^2 =$$

$$\frac{(p_1 k_1)(p_2 p_3)}{(p_1 k_2)(p_3 k_1)(p_4 - p_2)^4 x_{11}^4 x_{112}^4} \left\{ \begin{array}{l} x_{11}^2 x_{112}^2 (k_2 p_4)(p_3 p_1) \\ -2x_{11}^2 (x_{112} k_2)(x_{112} p_4)(p_3 p_1) \\ -2x_{112}^2 (x_{11} p_3)(x_{11} p_1)(k_2 p_4) \\ +4(x_{11} p_3)(x_{11} p_1)(x_{112} k_2)(x_{112} p_4). \end{array} \right\}$$

$$|\mathcal{M}_{2,1}(+, +, +, +, -, +)|^2 =$$

$$\frac{(p_3 p_2)(p_1 k_1)^2 (p_3 k_2)}{(p_2 k_1)(p_1 p_3)^2 (p_1 k_2)(p_4 - p_2)^4 x_{11}^4 x_{32}^4} \left\{ \begin{array}{l} x_{11}^2 x_{32}^2 (p_4 p_3) (p_2 p_1) \\ -2 x_{11}^2 (x_{32} p_2) (x_{32} p_1) (p_4 p_3) \\ -2 x_{32}^2 (x_{11} p_4) (x_{11} p_3) (p_2 p_1) \\ +4 (x_{11} p_4) (x_{11} p_3) (x_{32} p_2) (x_{32} p_1) \end{array} \right\}$$

$$|\mathcal{M}_{2,2}(+, -, +, -, -, +)|^2 =$$

$$\frac{(p_3 k_2)(p_1 k_1)}{(p_1 k_2)(p_3 k_1)(p_4 - p_2)^4 x_{11}^4 x_{32}^4} \left\{ \begin{array}{l} x_{11}^2 x_{32}^2 (p_4 p_1) (p_3 p_2) \\ -2 x_{11}^2 (x_{32} p_4) (x_{32} p_1) (p_3 p_2) \\ -2 x_{32}^2 (x_{11} p_3) (x_{11} p_2) (p_4 p_1) \\ +4 (x_{11} p_3) (x_{11} p_2) (x_{32} p_4) (x_{32} p_1) \end{array} \right\}$$

$$|\mathcal{M}_{3,1}(+, +, +, +, -, -)|^2 =$$

$$\frac{(p_4 p_3)(p_2 k_2)(p_1 k_1)}{(p_3 k_1)(p_4 k_2)(x_{11} - p_3)^4 x_{11}^4 x_{22}^4} \left\{ \begin{array}{l} x_{11}^2 x_{22}^2 (p_4 p_3) - 2 x_{11}^2 (x_{22} p_4) (x_{22} p_3) \\ -2 x_{22}^2 (x_{11} p_4) (x_{11} p_3) \\ +4 (x_{11} x_{22}) (x_{11} p_3) (x_{22} p_4) \end{array} \right\}$$

$$|\mathcal{M}_{3,2}(+, -, +, -, -, +)|^2 =$$

$$\frac{(p_1 k_1)(p_2 k_2)}{(p_4 k_2)(p_3 k_1)(x_{11} - p_3)^4 x_{11}^4 x_{22}^4} \left\{ \begin{array}{l} x_{11}^2 (x_{22} p_4) (p_4 p_3)^2 - 2x_{11}^2 (x_{22} p_4) (x_{22} p_3) (p_4 p_3) \\ - 2x_{22}^2 x_{11} p_4) (x_{11} p_3) (p_4 p_3) \\ + 4(x_{11} p_4) (x_{11} p_3) (x_{22} p_4) (x_{22} p_3). \end{array} \right\}$$

$$|\mathcal{M}_{4,1}(+, +, +, +, -, +)|^2 =$$

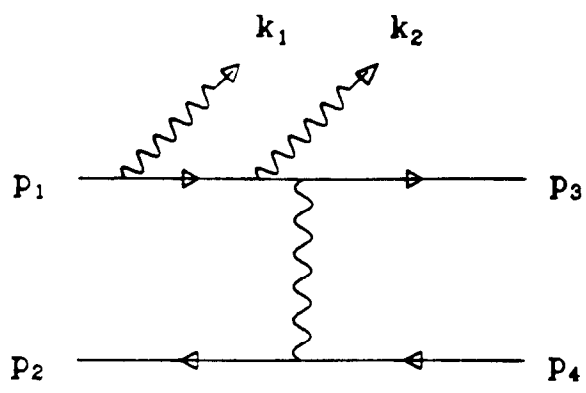
$$\frac{(p_1 k_1)(p_4 k_2)}{(p_3 k_1)(p_2 k_2)(x_{11} - p_3)^4 x_{11}^4 x_{42}^4} \left\{ \begin{array}{l} x_{11}^2 (p_4 p_2)^2 x_{42}^2 - 2x_{11}^2 (p_3 p_2) (p_3 x_{42}) (p_2 x_{42}) \\ - 2x_{42}^2 (x_{11} p_3) (x_{11} p_2) (p_3 p_2) \\ + 4(x_{11} p_3) (x_{11} p_2) (p_3 x_{42}) (p_2 x_{42}). \end{array} \right\}$$

$$|\mathcal{M}_{4,2}(+, -, +, -, -, -)|^2 =$$

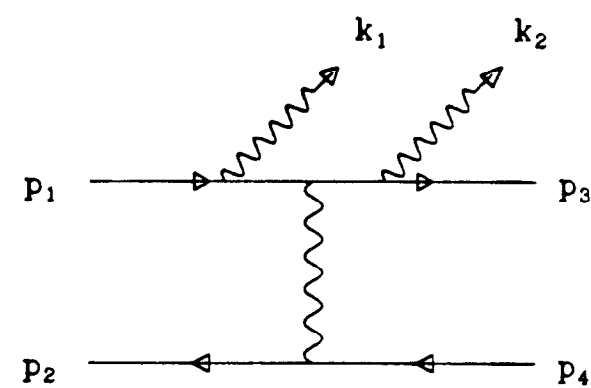
$$\frac{(p_4 k_2)(p_1 k_1)(p_2 p_3)}{(p_3 k_1)(p_2 k_2)(x_{11} - p_3)^4 x_{11}^4 x_{42}^4} \left\{ \begin{array}{l} x_{11}^2 x_{42}^2 (p_3 p_2) - 2x_{11}^2 (p_3 x_{42}) (p_2 x_{42}) \\ - 2x_{42}^2 (x_{11} p_3) (x_{11} p_2) \\ + 4(x_{11} p_3) (x_{11} x_{42}) (p_2 x_{42}). \end{array} \right\}$$

FIGURE 1

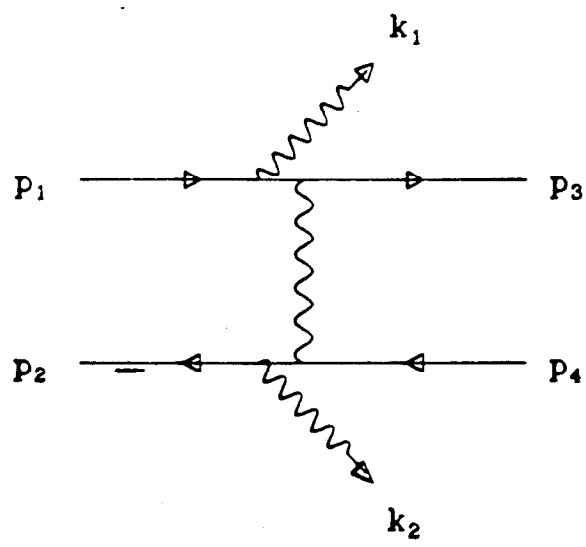
TYPE I



TYPE II



TYPE III



TYPE IV

